

The role of symmetry on interface states in magnetic tunnel junctions

C. Uiberacker and P. M. Levy

*Department of Physics, New York University,
4 Washington Place, New York, NY 10003*

(July 4, 2019)

Abstract

When an electron tunnels from a metal into the barrier in a magnetic tunnel junction it has to cross the interface. Deep in the metal the eigenstates for the electron can be labelled by the point symmetry group of the bulk but around the interface this symmetry is reduced and one has to use linear combinations of the bulk states to form the eigenstates labelled by the irreducible representations of the point symmetry group of the interface. In this way there can be states localized at the interface which control tunneling. The conclusions as to which are the dominant tunneling states are different from that conventionally found.

Magnetic tunnel junctions (MTJ's) are layered structures of the form ferromagnetic metal/insulator/ferromagnetic metal, and provide a very interesting area of basic research. The tunneling currents of MTJ's are very much influenced by the electronic structure around the interface between the electrodes and the insulating barrier. For example by inserting a few layers of Cu (dusting layers) between one of the ferromagnetic Co electrodes and the Al_2O_3 barrier it was found recently [1,2] that the TMR ratio is suppressed exponentially. Furthermore, by putting 1ML Cr between Co and the same barrier the TMR effect nearly vanishes but when inserting 3-5 ML of Co between the Cr layer and the barrier the TMR was restored again [3]. There have been theoretical attempts to model MTJ's with such dusting layers by using simple semiclassical models [4] and tight-binding schemes [5] that gave some insight on the role of Fermi surface mismatch between different metals and resulting quantum well states by defining a tunneling density of states. When quantum mechanics is used to study electrons in crystals it follows from the symmetry of the Hamiltonian that the energies and eigenstates can be labelled by the irreducible representations (IR's) of the space group. Because of the strong screening of the Fermi sea of a metal electrons are not aware of the interface until they are within 3-4 monolayers of it; therefore electron states inside a metal far from the interface are labelled by the IR's of the point group in the bulk. Close to the interface the electron states should be classified according to the IR's of the point group of the interface which is a subgroup of the point group in the bulk. In addition, states that are localized at the surface may form, e.g., on transition-metals with (100) surfaces [6]. These two features can be seen in Fig.(1) by comparing the density of states for minority electrons using as a basis the bulk eigenfunctions d_{z^2}, p_z, s (left figure) and the true eigenfunctions (right figure) at an Fe(100)/vacuum interface. Three layers away from the interface the true eigenfunctions are nearly identical to the bulk eigenfunctions, but in a range of 2 layers around the interface d_{z^2}, p_z, s cannot be used to describe the electron; rather one has to use appropriate linear combinations of these states to form the true eigenstates. We also note in these figures that the DOS peaks in the region of the interface and decay exponentially into the barrier but also decay inside the metal indicating that the minority states are localized at the interface. In this brief report we outline the procedure for identifying which states are primarily responsible for tunneling in MTJ's.

In order to analyze the electronic states in a MTJ one calculates the density of states (DOS) for it. Within a Green's function formalism and a single particle picture the DOS operator can be written as

$$\hat{\rho}(E; \delta) = \frac{1}{2\pi i} (\hat{G}^A - \hat{G}^R) = \frac{1}{2\pi i} (\hat{G}(E - i\delta) - \hat{G}(E + i\delta)) \quad (1)$$

by making use of the operators $\hat{G}^{R(A)}$ corresponding to the retarded and advanced Green's function. Here, i denotes the complex unit and the resolvent $\hat{G}(z)$ is defined by the equation

$$(z - \hat{H})\hat{G}(z) = \hat{I} \quad (2)$$

with z being a complex number, \hat{H} being the Hamiltonian and \hat{I} being the unit operator. Using the eigenfunctions $|\Phi_j\rangle$ of the Hamiltonian one can write the resolvent in the spectral representation and the DOS operator becomes

$$\hat{\rho}(E; \delta) = \frac{1}{\pi} \sum_j |\Phi_j\rangle\langle\Phi_j| \frac{\delta}{(E - E_j)^2 + \delta^2}; \quad \delta > 0 \quad . \quad (3)$$

Using the properties of $|\Phi_j\rangle\langle\Phi_j|$ it follows that $\hat{\rho}(E; \delta)$ is normal and therefore has real positive definite diagonal elements in any basis. Especially, in a real space representation expressed in an angular momentum basis the matrix elements

$$\rho(\mathbf{r}; E; \delta) = \sum_{LL'} \left(\frac{1}{\pi} \sum_j \Phi_{j,L}(r) \Phi_{j,L'}^*(r) \frac{\delta}{(E - E_j)^2 + \delta^2} \right) Y_L(\hat{\mathbf{r}}) Y_{L'}^*(\hat{\mathbf{r}}) \quad (4)$$

are real and positive for each value of r .

The MTJ we choose to investigate is Fe(100)/Vac/Fe(100) with an underlying b.c.c. lattice and we concentrated on the DOS around the surface in Fe(100)/Vac. For calculating the DOS we used the *ab-initio* spin-polarized scalar-relativistic Korringa-Kohn-Rostoker (KKR) multiple scattering formalism for layered systems [11] together with the local spin density approximation (LSDA) and the Gunnarsson-Lundqvist exchange-correlation potential [12]. To obtain short ranged structure constants, a screening formalism with a screening potential of 2.0 Ry was applied [11,13] and self-consistent potentials were evaluated within the atomic sphere approximation (ASA). First we calculated the potentials and exchange fields, where we used 16 points along a semi-circle in the complex energy plane with the points distributed on a Gaussian mesh and 45 k_{\parallel} points in the irreducible surface Brillouin zone (ISBZ). The vacuum was simulated by six layers of empty atomic spheres which have an underlying b.c.c. lattice structure. For calculating the DOS we choose an imaginary part of $\delta = 5 \times 10^{-4}$ Ry and took 1830 k_{\parallel} points in the ISBZ for the minority and majority spin-channel.

In KKR for layered systems the arrangement of atoms within each layer is decomposed into Wigner-Seitz cells. An arbitrary point \mathbf{r}_n^p is then uniquely described by the origin of cell n in layer p , \mathbf{R}_n^p , and the position \mathbf{r} inside this cell and therefore $\mathbf{r}_n^p = \mathbf{R}_n^p + \mathbf{r}$. In the ASA each cell is then replaced by a sphere of equal volume and the potential inside the cell is assumed to be spherically symmetric. It follows that the eigenfunctions of the Hamiltonian inside a given cell can be written as a series in angular momentum with expansion coefficients depending only on the distance from the origin of the cell. Then the Green's function can be written as

$$G(\mathbf{r}_n^p, \mathbf{r}_m'^q; E + i\delta) = \sum_{LL'} \{ Z_l^{n;p}(r) \tau_{LL'}^{nm;pq} Z_{l'}^{m;q}(r') - \delta_{nm} \delta_{pq} \delta_{LL'} [Z_l^{n;p}(r) J_l^{n;p}(r') \theta(r' - r) + J_l^{n;p}(r) Z_l^{n;p}(r') \theta(r - r')] \} Y_L(\hat{\mathbf{r}}) Y_{L'}^*(\hat{\mathbf{r}}') \quad , \quad (5)$$

by using $L = (l, m)$ as a shorthand notation, in terms of the scattering path operator $\tau_{LL'}^{nm;pq}$ and the regular solutions $Z_l^{n;p}(r)$ and the irregular solution $J_l^{n;p}(r)$ of the Schrödinger equation which all depend implicitly on $E + i\delta$ [11,13]. Using the fact that the Hamiltonian is hermitean it immediately follows that $\hat{G}(E - i\delta) = \hat{G}^\dagger(E + i\delta)$ and inserting this into Eqn.(1) yields

$$\begin{aligned} \rho(\mathbf{r}_n^p, \mathbf{r}_m'^q; E; \delta) &= \frac{1}{2\pi i} \{ [G(\mathbf{r}_m'^q, \mathbf{r}_n^p; E + i\delta)]^* - G(\mathbf{r}_n^p, \mathbf{r}_m'^q; E + i\delta) \} \\ &= \frac{1}{2\pi i} \sum_{LL'} \{ [G_{L'L}^{mn;qp}(r', r)]^* - G_{LL'}^{nm;pq}(r, r') \} Y_L(\hat{\mathbf{r}}) Y_{L'}^*(\hat{\mathbf{r}}') \end{aligned} \quad (6)$$

and the diagonal matrix elements are

$$\begin{aligned}
\rho(\mathbf{r}_n^p; E; \delta) &= \sum_{LL'} \rho_{LL'}^{n;p}(r; E; \delta) Y_L(\hat{\mathbf{r}}) Y_{L'}^*(\hat{\mathbf{r}}) \\
&= \sum_{LL'} \left\{ \left[Z_{l'}^{n;p}(r)^* \tau_{L'L}^{nn;pp*} Z_l^{n;p}(r)^* - Z_l^{n;p}(r) \tau_{LL'}^{nn;pp} Z_{l'}^{n;p}(r) \right] / 2\pi i \right. \\
&\quad \left. + \text{Im} [Z_l^{n;p}(r) J_l^{n;p}(r)] \right\} Y_L(\hat{\mathbf{r}}) Y_{L'}^*(\hat{\mathbf{r}})
\end{aligned} \tag{7}$$

It is very common to calculate the L -resolved integrated DOS (simply called L -resolved ‘density of states’) which can be obtained from the previous equation as follows

$$\text{Tr} \hat{\rho}(E; \delta)|_{L;n;p} = \int d\mathbf{r} \rho_{LL'}^{n;p}(\mathbf{r}; E; \delta) \tag{8}$$

The matrix of expansion coefficients in Eq.(7) for a fixed cell n in layer p , which can be defined in terms of its components by

$$\boldsymbol{\rho}^{n;p}(r; E; \delta) = \{\rho_{LL'}^{n;p}(r; E; \delta)\} \quad , \tag{9}$$

will be invariant under all operations of the point group. Due to the fact that the point group is a subgroup of the rotation-reflection group $\mathcal{O}(3)$ the basis functions of the IR’s of the point group will be linear combinations of spherical harmonics. Moreover it can occur that in the truncated (l,m) basis used for calculations, which was up to $l = 2$ in our case, several spherical harmonics belong to the same IR and therefore $\boldsymbol{\rho}^{n;p}(r; E; \delta)$ will have off-diagonal elements connecting these functions. By grouping these basis functions that belong to the same IR $\boldsymbol{\rho}^{n;p}(r; E; \delta)$ becomes block-diagonal with one block per IR. Now each block that contains more than one basis function has to be diagonalized to find the contributions $\rho_j^{n;p}(r; E; \delta)$ belonging to the given IR, where j labels the eigenfunctions of \hat{H} . If the quantization axis is chosen normal to the interface (\mathbf{z} -direction) then at least all states $(l, m = 0)$, which are functions of \mathbf{z} only, will belong to the identity representation (they are invariant under all operations of the group) and the corresponding eigenfunctions will be linear combinations of these states. This is valid for *all* 2D points groups and is therefore very general. Due to the fact that $\boldsymbol{\rho}^{n;p}(r; E; \delta)$ depends on r and p the transformation that diagonalize it will also depend on r and p and therefore the basis formed by the eigenfunctions (‘eigenbasis’) will gradually change in a MTJ when going from the metal into the barrier.

In Fe(001)/Vac the underlying crystal structure is b.c.c. and for the (001) surface the 2D lattice in the layers parallel to the surface is quadratic. The point group of the 2D lattice is therefore the group C_{4v} (Schönflies notation) or $4mm$ (International notation) and it has 5 irreducible representations Δ_i , $i = 1, \dots, 5$ where the first four are 1D and the 5th is 2D [8]. For an angular momentum basis up to $l = 2$, Δ_2 is not realized. Δ_1 is the identity representation which is realized by s , p_z and d_{z^2} independently and we will concentrate on the mixing of these functions.

In Figs.(2)-(4) we plot the L -resolved integrated DOS defined in Eq.(8) for the surface layer and the first and second vacuum layer against the energy for the functions belonging to Δ_1 . Furthermore, we plot the total Δ_1 contribution in the bulk in order to see if some states that occur at the surface do not occur in the bulk and therefore may be localized. Majority contributions are plotted with the correct sign and minority contribution with a reversed sign. The left graph shows the DOS in the (l, m) basis and the right graph shows the DOS in the eigenbasis and we will concentrate on the (l, m) basis first. Looking at the left part of

Fig.(2) one can indeed see that at 1.6 eV below the Fermi Energy E_f in the majority DOS and around E_f in the minority DOS there are states that have no counterpart in the bulk. To find out if these states are localized we have a look at Fig.(3) and Fig.(4) which show the DOS in the vacuum. Indeed, one finds a state at $E_f-1.6\text{eV}$ in the majority DOS and around E_f in the minority DOS which has a similar shape as the one at the surface layer, however we note it is largely of s -character whereas the state in Fig.(2) was mainly of d_{z^2} character. From that one could conclude that the state found at the surface of the metal does not continue into the vacuum and is therefore not localized. Moreover, in Fig.(4) it seems these contributions consist of two states with s and p_z character. However, these conclusions are *wrong* because when we look at the DOS in the eigenbasis (right part of Fig.(2)) we see that the peaks mentioned above result from one eigenstate that extends from the surface into the vacuum. If this were not the case there would be a state at the surface of Fe that would be damped almost completely at the first vacuum layer and one in the vacuum that is damped similarly at the surface of Fe, and at some point in between Fe and vacuum the DOS from these states must cross. This, however, is not possible because for all 2D point groups the eigenfunctions belonging to Δ_1 span 1D invariant spaces and therefore degenerate eigenvalues cannot occur in the Δ_1 block of ρ ; otherwise an invariant space of dimension ≥ 2 would exist. To illustrate this fact we plotted in Fig.(5) the component resolved DOS for the minority spin channel versus r by taking the diagonal elements of $\rho^{n;p}(r; E; \delta)$ in the (l, m) basis (left graph) and in the eigenbasis (right graph). $r = 0$ denotes the center of a cell in the surface layer and the vertical broken lines denotes the boundaries between layers when going from the surface into the vacuum. One can see that when transforming from the (l, m) basis to the eigenbasis any crossings of states occurring between the surface and the first vacuum layer are removed. The resulting eigenstates exist at the surface *and* in the vacuum. While we have focused on the minority states, the majority DOS versus r behaves qualitatively in the same way.

The discontinuity of the eigenstates across the boundaries of layers in Fig.(5) comes from the fact that in the ASA the DOS is symmetric around the center of the cell in a layer and therefore is the same on the left and right boundary in Fig.(5). By using a full potential calculation these discontinuities are removed, but otherwise it should qualitatively yield the same results.

A typical wavelength of an electron at E_f is in the order of the layer spacing and it is only meaningful to present the average of the DOS over a given layer, therefore we plot the integrated DOS for each eigenstate on each layer in Fig.(1). Besides the facts discussed in the introduction one can see that different states within Δ_1 have equal decay rates in vacuum. This is also observed for states belonging to Δ_5 and it follows that each IR has one decay rate which then does not depend on the basis used. The different decay rates for the different IR's have already been pointed out and investigated by others [9,10]. However, when they did their analysis they only took the trace over each block in $\int_{\text{cell}} dr \rho^{n;p}(r; E; \delta)$, obtaining the total contribution from each IR, and did not analyze the functions within a block to find the true eigenfunctions of the Hamiltonian (which are linear combinations of IR basis functions) that change when going from the electrode into the barrier.

For completeness we want to mention that the states $d_{x^2-y^2}$ and d_{xy} which belong to Δ_3 and Δ_4 will already be the eigenstates of the Hamiltonian but the 2D IR Δ_5 is realized by two sets of basis functions, namely (d_{xz}, d_{yz}) and (p_x, p_y) . Functions that belong to the

same row of the same IR will mix and this applies to the pairs d_{xz}, p_x and d_{yz}, p_y . Both pairs form the same pair of eigenstates and the two corresponding eigenvalues are twofold degenerate. The contribution from $\Delta_3, \dots, \Delta_5$ to the surface state found above is about an order of magnitude smaller than from the eigenfunctions belonging to Δ_1 near the surface and becomes negligible in large barriers due to their larger decay.

In summary we defined a density of states operator and its real space representation and showed that it is very useful for analyzing the electronic states in a magnetic tunnel junction. We showed that especially the point group of the layers parallel to the interface between the electrodes and the barrier and its irreducible representations can give some insight by making the DOS matrix defined in Eq.(9) block-diagonal. But we stress that finding the eigenbasis within these blocks cannot be provided by symmetry but has to be found by solving a secular equation. Concentrating on the identity representation gives us a better understanding how localized states at (001) and (111) surfaces/interfaces in the cubic Bravais lattices can occur and that they will be of $(s, p_z) - d_{z^2}$ character *independent* of the actual material used for the electrode and the barrier (the \mathbf{z} direction is chosen normal to the surface/interface). The general feature of $s - d_{z^2}$ surface states in bcc (001) surfaces of different materials found by experiment has been mentioned in [6]. Like others, see e.g. [10], they use the bulk band structure and project it onto the face corresponding to the interface when discussing these states. This procedure implicitly uses a fixed (l, m) basis and not the eigenbasis, therefore it cannot explain how these states are formed. Finally we want to point out that states localized at the electrode/barrier interface play a crucial role in tunneling, and in the case of Fe/vacuum alter one's expectations about the spin polarization of the tunneling current. While one would argue on the basis of the itinerant (bulk) states in the junction that the current has a majority spin polarization, electrons can be scattered into the localized states at the interface and thereby reverse the spin-polarization of the tunneling current. This is reflected in the DOS at the interface around E_f , see Fig.(2) .

This work was supported by the Defense Advanced Research Projects Agency and the Office of Naval Research (Grant No. N00014-96-1-1207 and Contract Nos. MDA972-96-C-0014, and MDA972-99-C-0009).

REFERENCES

- [1] P. LeClair, H. J. M. Swagten, J. T. Kohlhepp, and W. J. M. de Jonge, *Appl. Phys. Lett.* **76**, 3783 (2000)
- [2] P. LeClair, H. J. M. Swagten, J. T. Kohlhepp, R. J. M. van de Veerdonk, and W. J. M. de Jonge, *Phys. Rev. Lett.* **84**, 2933 (2000)
- [3] P. LeClair, J. T. Kohlhepp, H. J. M. Swagten, and W. J. M. de Jonge, to be published in *J. Appl. Phys.*
- [4] S. Zhang and P. M. Levy, *Phys. Rev. Lett.* **81**, 5660 (1998)
- [5] J. Mathon and A. Umerski, *Phys. Rev. B* **60**, 1117 (1999)
- [6] J. A. Stroscio, D. T. Pierce, A. Davies, R. J. Celotta, and M. Weinert, *Phys. Rev. Lett.* **75**, 2960 (1995).
- [7] P. Zahn, J. Binder, I. Mertig, R. Zeller and P. H. Dederichs, *Phys. Rev. Lett.* **80**, 4309 (1998)
- [8] M. Hamermesh, 'Group Theory', Addison-Wesley, Reading (1964); C. J. Bradley and A. P. Cracknell, 'The Mathematical Theory of Symmetry in Solids', Oxford University Press, Oxford (1972)
- [9] W. H. Butler, X.-G. Zhang, T. C. Schulthess, and J. M. MacLaren, *Phys. Rev. B* **63**, 092402 (2001)
- [10] Ph. Mavropoulos, N. Papanikolaou, and P. H. Dederichs, *Phys. Rev. Lett.* **85**, 1088 (2000)
- [11] L. Szunyogh, B. Újfalussy, P. Weinberger, and J. Kollár, *Phys. Rev. B* **49**, 2721 (1994).
- [12] O. Gunnarsson and B. I. Lundqvist, *Phys. Rev. B* **13**, 4274 (1976).
- [13] R. Zeller, P. H. Dederichs, B. Újfalussy, L. Szunyogh, and P. Weinberger, *Phys. Rev. B* **52**, 8807 (1995).

FIGURES

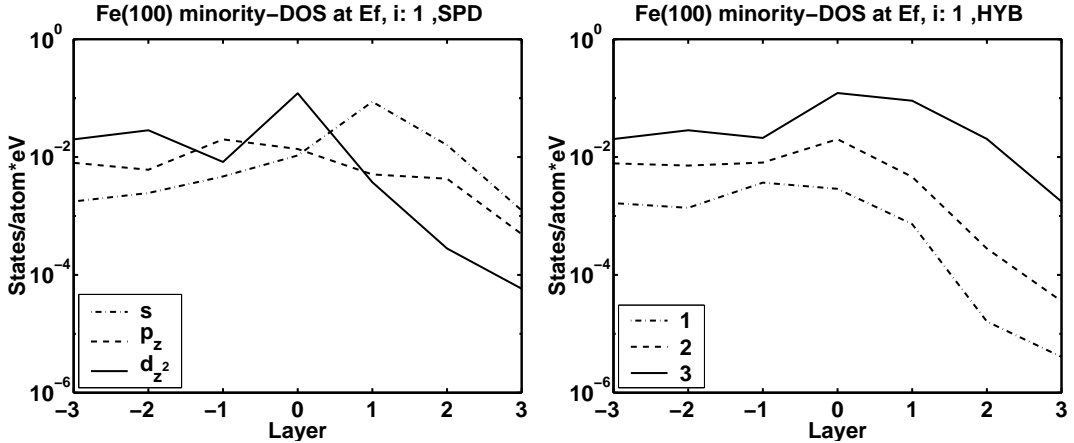


FIG. 1. Δ_1 contribution to the integrated DOS at the Fermi Energy plotted on each layer in the IR basis (left) and eigenbasis (right) for minority states. Layer 0 denotes the surface layer and layers > 0 denote vacuum.

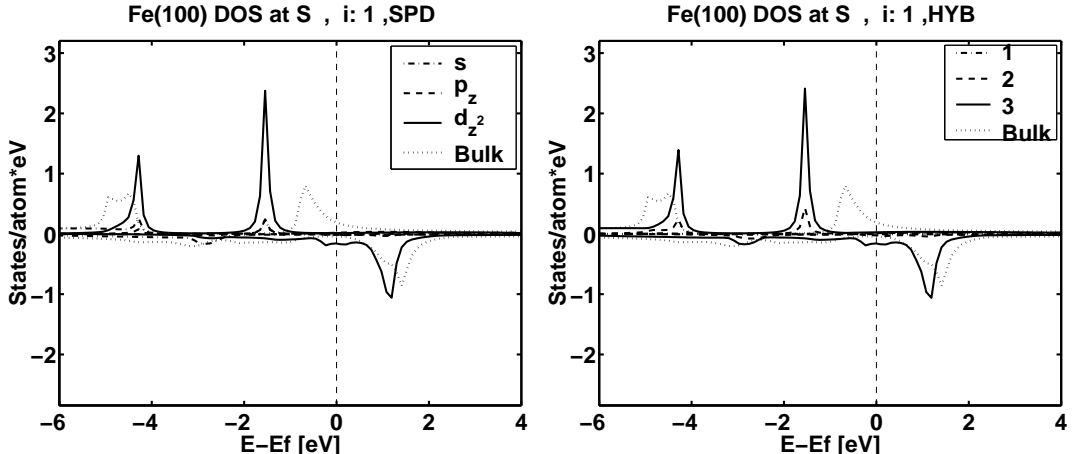


FIG. 2. Δ_1 contribution to the integrated density of states plotted versus energy for the surface layer of $\text{Fe}(100)|\text{Vac}$ in the IR basis (left) and the eigenbasis (right). The minority DOS is plotted with reversed sign.

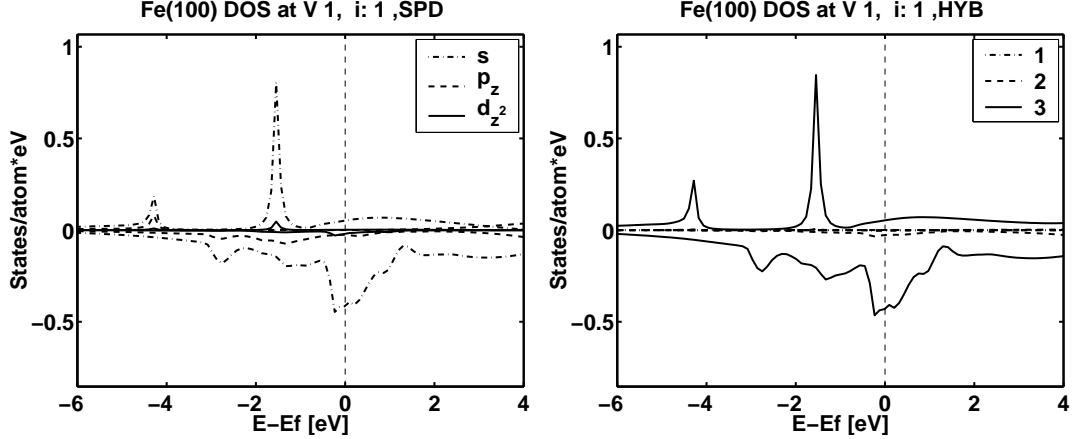


FIG. 3. Δ_1 contribution to the integrated density of states plotted versus energy for the first vacuum layer of $\text{Fe}(100)|\text{Vac}$ in the IR basis (left) and the eigenbasis (right). The minority DOS is plotted with reversed sign and 5 times enlarged.

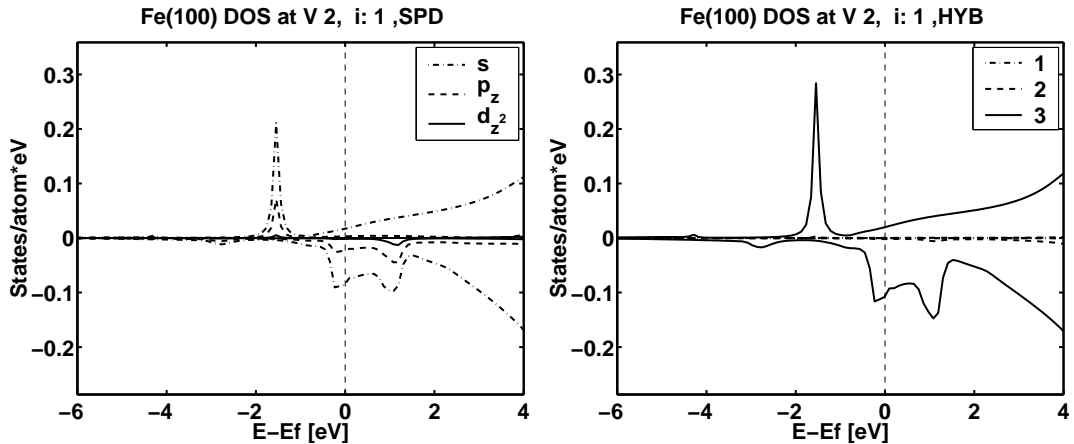


FIG. 4. Δ_1 contribution to the integrated density of states plotted versus energy for the second vacuum layer of $\text{Fe}(100)|\text{Vac}$ in the IR basis (left) and the eigenbasis (right). The minority DOS is plotted with reversed sign and 5 times enlarged.

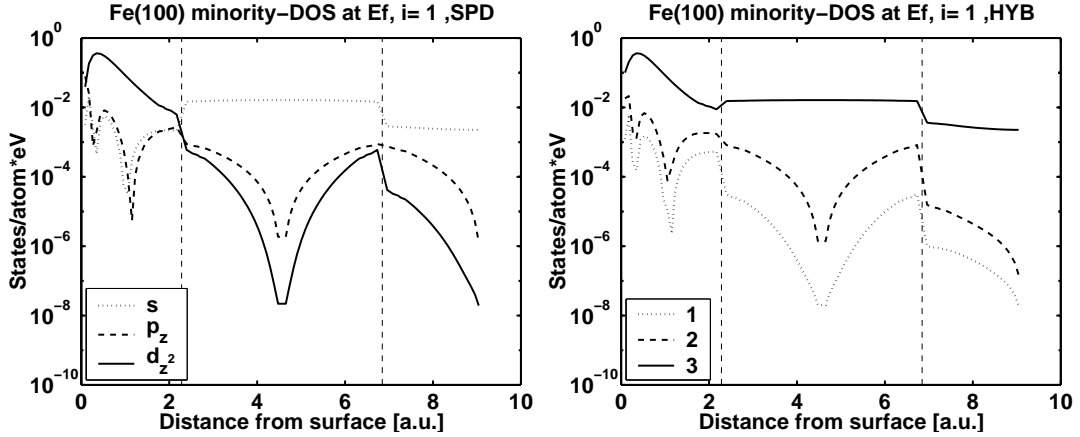


FIG. 5. Δ_1 contribution to the minority DOS matrix $\rho(r; E; \delta)$ at the Fermi Energy plotted versus r in the IR basis (left) and the eigenbasis (right). $r = 0$ denotes the center of the cell in the surface layer and r is measured in the direction to the vacuum.